

# Phenomenological study on the decay widths of $\Upsilon(nS) \rightarrow \bar{d}^*(2380) + X^*$

Chao-Yi Lü(吕超一)<sup>1,2;1)</sup> P. Wang(王平)<sup>2,3;2)</sup> Y. B. Dong(董宇兵)<sup>2,3</sup>P. N. Shen(沈彭年)<sup>2,3</sup> Z. Y. Zhang(张宗烨)<sup>2,3</sup> D. M. Li(李德民)<sup>1</sup><sup>1</sup> Department of Physics, Zhengzhou University, Zhengzhou, Henan 450001, China<sup>2</sup> Institute of High Energy Physics, Chinese Academy of Sciences, Beijing 100049, China<sup>3</sup> Theoretical Physics Center for Science Facilities, Chinese Academy of Sciences, Beijing 100049, China

**Abstract:** The decay widths of  $\Upsilon(nS) \rightarrow \bar{d}^*(2380) + X$  with  $n=1,2,3$  are studied in a phenomenological way. With the help of crossing symmetry, the decay widths are obtained by investigating the imaginary part of the forward scattering amplitudes between  $d^*$  and  $\Upsilon(nS)$ . The wave functions of  $d^*$  and deuteron obtained in previous studies are used for calculating the amplitude. The interaction between  $d^*$  ( $d$ ) and  $\Upsilon$  is governed by the quark-meson interaction, where the coupling constant is determined by fitting the observed widths of  $\Upsilon(nS) \rightarrow \bar{d} + X$ . The numerical results show that the decay widths of  $\Upsilon(nS) \rightarrow \bar{d}^* + X$  are about 2–10 times smaller than that of  $\bar{d} + X$ . The calculated momentum of  $\bar{d}^*$  is in the range 0.3–0.8 GeV. Therefore, it is very likely that one can find  $\bar{d}^*(2380)$  in these semi-inclusive decay processes.

**Keywords:** Upsilon decay, SU(3) chiral quark model,  $\bar{d}^*(2380)$  production

**PACS:** 13.20.Gd, 21.10.Tg, 21.60.-n      **DOI:** 10.1088/1674-1137/42/6/064102

## 1 Introduction

In recent years, a resonance-like structure named  $d^*(2380)$  was observed by the WASA-at-COSY collaborations in  $p\bar{n} \rightarrow d\pi^0\pi^0$ ,  $p\bar{n} \rightarrow d\pi^+\pi^-$ , when they studied the ABC effect [1, 2]. Later, this particle was confirmed in series of reactions, such as  $p\bar{n} \rightarrow p\bar{n}\pi^0\pi^0$ ,  $p\bar{n} \rightarrow p\bar{p}\pi^-\pi^0$ ,  $p\bar{d} \rightarrow {}^3He\pi^0\pi^0$ ,  $p\bar{d} \rightarrow {}^3He\pi^+\pi^-$ , etc [3–8]. The analysis of experimental data shows that  $d^*$  has a mass of 2380 MeV, a decay width of about 70 MeV, and its spin, isospin, and parity are  $I(J^P)=0(3^+)$  [9]. Since its mass is about 70 MeV higher than the  $\Delta N\pi$  threshold and about 80 MeV lower than the  $\Delta\Delta$  threshold, the threshold effect is small for this particle. Because of its non-conventional features of a narrow width plus a large binding energy with respect to the  $\Delta\Delta$  threshold, the structure of  $d^*$  has attracted attention.

In fact, theoretical investigations for such a state started more than 50 years ago. After the publication of the newly observed data, many theoretical calculations with various structural models have been carried out. Among them, two major structural models that can basically explain all the measured data have been investigated intensively. One of the models considers an

exotic compact hexaquark-dominated structure [10–16], and the other uses a quasi-molecular resonance of  $\Delta N\pi$  (or  $D_{12}\pi$ ) [17, 18]. However, apart from searching for new physical quantities to distinguish different structural assumptions, proposing a new accessible physical process other than nuclear reactions or scattering processes to confirm the existence of the  $d^*$  state is extremely important.

It is well-known that in the strong decay of heavy quarkonium, the heavy quark annihilates with its anti-particle and new quark-antiquark pairs are created. For  $\Upsilon$ , it can decay into a wide variety of combinations of hadrons [19]. Among these hadronic decay modes, an interesting mode is the semi-inclusive anti-deuteron ( $\bar{d}$ ) production processes  $\Upsilon(nS) \rightarrow \bar{d} + X$ . This is because  $\bar{d}(\bar{d}^*)$  and  $d(d^*)$  are bottomless baryons. The observation of  $\bar{d}(\bar{d}^*)$  in the  $\Upsilon(nS)$  decays implies the existence of  $d(d^*)$  in the same process. Since the mass of  $\Upsilon(nS)$  is larger than the mass of the  $d^*\bar{d}^*$  pair, the phase space is large enough for  $\Upsilon(nS)$  to decay into  $\bar{d}^*$  (or  $d^*$ ) plus other hadrons. Therefore, it is natural to think that  $\bar{d}^*(2380)$  is quite possible to be produced in the semi-inclusive decays of  $\Upsilon(nS)$ . In this paper, we will start from the  $\Upsilon(nS) \rightarrow \bar{d} + X$  decays. By fitting the decay

Received 22 March 2018, Published online 16 May 2018

\* Supported by National Natural Sciences Foundations of China (11475186, 11475192, 11521505, 11565007), the Sino-German CRC 110 "Symmetries and the Emergence of Structure in QCD" project by NSFC (11621131001), the Key Research Program of Frontier Sciences, CAS, (Y7292610K1) and the IHEP Innovation Fund (Y4545190Y2)

1) E-mail: lvcy@ihep.ac.cn

2) E-mail: pwang4@ihep.ac.cn

©2018 Chinese Physical Society and the Institute of High Energy Physics of the Chinese Academy of Sciences and the Institute of Modern Physics of the Chinese Academy of Sciences and IOP Publishing Ltd

widths of these processes, we can fix the unknown parameters required in the  $\Upsilon \rightarrow \bar{d}^* + X$  calculation and then estimate the decay widths (and/or numbers of events) of the latter decay process.

The paper is organized as follows. In Section 2, the formulism for the decay widths of the  $\Upsilon(nS) \rightarrow \bar{d}(\bar{d}^*) + X$  processes is briefly introduced. Numerical results and discussions are presented in Section 3. Finally, a short summary is given in Section 4.

## 2 Brief formulism

In this section, we will study the decay widths for  $\Upsilon(nS) \rightarrow \bar{d}^*(2380) + X$ . With the crossing symmetry, we investigate the scattering between  $d^*(2380)$  and  $\Upsilon(nS)$ . By virtue of the optical theorem, the decay widths can be obtained by calculating the imaginary part of the forward scattering amplitudes of  $d^*(2380) + \Upsilon(nS) \rightarrow d^*(2380) + \Upsilon(nS)$ . In these specific elastic scattering processes, because the quarks in  $d^*$  and  $\Upsilon$  belong to a completely different type, the exchange of quarks from different hadrons cannot occur, while the exchange of gluon between the quarks from different hadrons also does not contribute. The only possible interaction between  $d^*$  and  $\Upsilon$  is the  $s$ -channel meson exchange. Therefore, in the study of the  $d^*(d) - \Upsilon(nS)$  scattering, we adopt a constituent quark model with a meson exchange potential, where we assume that the B-meson exchange dominates, to calculate the elementary process  $\bar{b} + u(d) \rightarrow \bar{b} + u(d)$ . The relevant Feynman diagram is shown in Fig. 1.

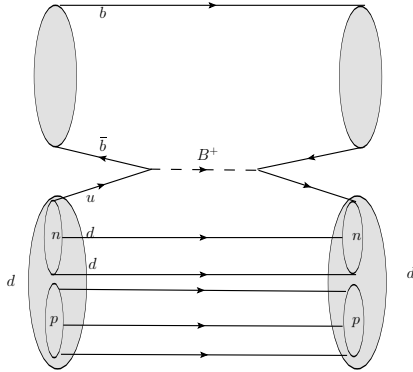


Fig. 1. The Feynman diagram of  $\Upsilon + d \rightarrow \Upsilon + d$  forward scattering.

In this figure, the interaction between  $\Upsilon$  and  $d(d^*)$  is governed by the quark-meson interaction. The corresponding Lagrangian can be written as

$$\mathcal{L} = ig_{\bar{b}qB}\bar{\psi}_{\bar{b}}\gamma_5\psi_q B, \quad (1)$$

where  $g_{\bar{b}qB}$  is the coupling constant, and  $\psi_q$ ,  $\psi_{\bar{b}}$ , and  $B$  denote the fields of the light quark  $q$ , anti-bottom quark  $\bar{b}$  and B meson, respectively. To restrict the value of the

coupling constant  $g_{\bar{b}qB}$ , we first study the forward scattering of  $d + \Upsilon \rightarrow d + \Upsilon$  (Fig. 1). The scattering amplitude can be written as

$$\mathcal{M} = g_{\bar{b}qB}^2 \Psi_{\Upsilon}^* \Psi_d^* \bar{u}(p_u) \gamma_5 v(p_{\bar{b}}) \frac{1}{q^2 - m_B^2 + imF} \times \bar{v}(p_{\bar{b}}) \gamma_5 u(p_u) \Psi_d \Psi_{\Upsilon},$$

where  $\Psi_{\Upsilon}$  and  $\Psi_d$  are the wave functions of the  $\Upsilon(nS)$  and deuteron, respectively.  $u(p_u)$ ,  $\bar{u}(p_u)$ ,  $\bar{v}(p_{\bar{b}})$  and  $v(p_{\bar{b}})$  represent the spinors of the  $u(d)$ -quark and  $\bar{b}$ -quark in the initial and final states, respectively. The wave functions of  $\Upsilon(nS)$  can be obtained by solving the Schrödinger equation with a Cornell potential [20–23]. The obtained masses for the  $1S$ ,  $2S$  and  $3S$  states are 9.46 GeV, 10.02 GeV and 10.34 GeV, respectively, which are quite close to the experimental data.

In the quark cluster model, the wave function of the deuteron in the quark degrees of freedom can simply be expressed as

$$\Psi_d = \mathcal{A} [\phi_N(\vec{\rho}_1, \vec{\lambda}_1) \phi_N(\vec{\rho}_2, \vec{\lambda}_2) \eta_{NN}^{l=0}(\vec{R}) \zeta_d]_{(SI)=(10)} \quad (2)$$

where  $\mathcal{A}$  is the total anti-symmetrization operator,  $\phi_N$  is the internal wave function of nucleon,  $\eta_{NN}^{l=0}$  represents the relative wave function in  $S$ -wave, which is determined by the dynamical calculation of the system with the (extended) chiral SU(3) constituent quark model, and  $\zeta_d$  stands for the spin-isospin wave function in the hadronic degrees of freedom (more details can be found in Ref. [24]). As commonly used, the internal wave function of the nucleon can be taken as

$$\phi_N = \frac{1}{\sqrt{2}} [\chi_{\rho} \psi_{\rho} + \chi_{\lambda} \psi_{\lambda}] \Phi_N(\vec{\rho}, \vec{\lambda}), \quad (3)$$

with  $\chi_{\rho}$  ( $\chi_{\lambda}$ ) and  $\psi_{\rho}$  ( $\psi_{\lambda}$ ) being the symmetric (anti-symmetric) wave functions in the spin and isospin spaces,  $\Phi(\vec{\rho}, \vec{\lambda})$  the spatial wave function and  $\rho$  and  $\lambda$  the Jacobi coordinates. In the same way, the wave function of  $d^*$  can be abbreviated to the form

$$\Psi_{d^*} = \mathcal{A} [\phi_{\Delta}(\vec{\rho}_1, \vec{\lambda}_1) \phi_{\Delta}(\vec{\rho}_2, \vec{\lambda}_2) \eta_{\Delta\Delta}^{l=0}(\vec{R}) \zeta_{\Delta\Delta} + \phi_{C_8}(\vec{\rho}_1, \vec{\lambda}_1) \phi_{C_8}(\vec{\rho}_2, \vec{\lambda}_2) \eta_{C_8C_8}^{l=0}(\vec{R}) \zeta_{C_8C_8}]_{(SI)=(30)}, \quad (4)$$

where  $\mathcal{A}$  is the total anti-symmetrization operator,  $\phi_{\Delta}$  and  $\phi_{C_8}$  denote the inner cluster wave functions of  $\Delta$  and  $C_8$  (color-octet particle) in the coordinate space,  $\eta_{\Delta\Delta}^{l=0}$  and  $\eta_{C_8C_8}^{l=0}$  represent the  $S$ -wave relative wave functions between  $\Delta\Delta$  and  $C_8C_8$  clusters (the  $D$ -wave components are negligibly small), and  $\zeta_{\Delta\Delta}$ ,  $\zeta_{C_8C_8}$  stand for the spin-isospin wave functions in the hadronic degrees of freedom in the corresponding channels, respectively. The channel wave function can be defined as

$$\chi_{\Delta\Delta(C_8C_8)}^{eff, l=0}(\vec{R}) = \langle \phi_{\Delta(C_8)}(\vec{\rho}_1, \vec{\lambda}_1) \phi_{\Delta(C_8)}(\vec{\rho}_2, \vec{\lambda}_2) | \Psi_{d^*} \rangle. \quad (5)$$

Therefore, for simplicity, the wave function of  $d^*$  can be rewritten as

$$\Psi_{d^*} \cong [\phi_\Delta(\vec{p}_1, \vec{\lambda}_1) \phi_\Delta(\vec{p}_2, \vec{\lambda}_2) \chi_{\Delta\Delta}^{\text{eff},l=0}(\vec{R}) \zeta_{\Delta\Delta} + \phi_{C_8}(\vec{p}_1, \vec{\lambda}_1) \phi_{C_8}(\vec{p}_2, \vec{\lambda}_2) \chi_{C_8C_8}^{\text{eff},l=0}(\vec{R}) \zeta_{C_8C_8}]_{(SI)=(30)}.$$

We should emphasize that our treatment for the wave function of  $d^*$  is just an approximation for reducing tedious and almost inoperable calculations and making the two components orthogonal. The obtained effective relative wave function can reasonably contain most of the effect of anti-symmetrization of the wave function of  $d^*$  shown in Eq. (4). The effective wave function is obtained by projecting onto the physical base, and further described by the sum of four Gaussian functions.

$$\chi_{\Delta\Delta(C_8C_8)}^{\text{eff},l=0}(\vec{R}) = \sum_{i=1}^4 c_i \exp\left(-\frac{\vec{R}^2}{2b_i^2}\right). \quad (6)$$

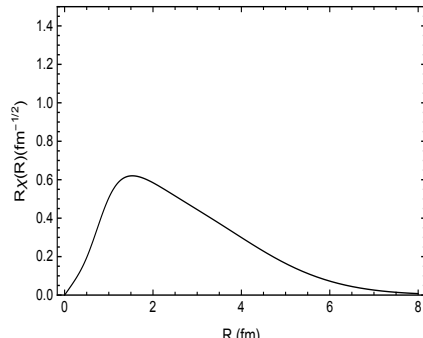
It should be noticed that the quantum numbers for the color-octet  $C_8$ -cluster and the color-singlet  $\Delta$ -cluster in  $d^*$  are different. For the  $C_8$ -cluster,  $S=3/2, I=1/2, C=(11)$ , while for the  $\Delta$ -cluster,  $S=3/2, I=3/2, C=(00)$ , where  $S$ ,  $I$  and  $C$  denote the spin, isospin and color, respectively. It should be specially mentioned that these two channel wave functions are orthogonal to each other and contain all the effects of the totally anti-symmetrization implicitly. The details can be found in Refs. [12–14, 16, 24].

On the other hand, the data published by the PDG [19] show that the width of the  $B$  meson is very small. Therefore, the propagator can be written as

$$\frac{1}{q^2 - m_B^2 + i\Gamma} \approx \frac{1}{q^2 - m_B^2 + i\epsilon} \rightarrow -2\pi i \delta(q^2 - m_B^2). \quad (7)$$

Then, the imaginary part of the amplitude is expressed as

$$\text{Im}\mathcal{M} = - \int d\Pi 2\pi g_{\bar{b}qB}^2 \Psi_Y^* \Psi_d^* \bar{u}(p_u) \gamma_5 v(p_b) \times \bar{v}(p_b) \gamma_5 u(p_u) \Psi_d \Psi_Y \delta(q^2 - m_B^2), \quad (8)$$



where  $d\Pi$  is an integral measure, including  $d\vec{p}_\rho$ ,  $d\vec{p}_\lambda$ ,  $d\vec{p}_\eta$  and  $d\vec{p}_R$  for the internal momenta in the nucleon, internal momentum of  $\Upsilon$  and relative momentum between nucleons, respectively. The momenta  $\vec{p}_b$ ,  $\vec{p}_u$  and  $\vec{q}=\vec{p}_b+\vec{p}_u$  are related to these momenta and the momentum  $\vec{p}_d$  of the deuteron through the Jacobian transformation shown in Appendix A. The forward scattering condition requires that the momenta and quantum numbers of quarks in the initial and final states do not change.

With the optical theorem, the semi-inclusive decay width of  $\Upsilon \rightarrow \bar{d}+X$  can be calculated by

$$d\Gamma = \frac{1}{m_\Upsilon} \left( \frac{d\vec{p}_d}{(2\pi)^3} \frac{1}{2E_d} \right) \times \text{Im}\mathcal{M}(\Upsilon+d \rightarrow \Upsilon+d). \quad (9)$$

Integrating over the possible range of  $p_d$ , the decay widths of  $\Upsilon(nS)$  to  $\bar{d}+X$  can be obtained. In the final step, the upper limit of the  $p_d$  integration is determined by the four-momentum conservation

$$\sqrt{\vec{p}_d^2 + m_d^2} + \sqrt{\vec{p}_d^2 + M_X^2} = m_\Upsilon. \quad (10)$$

with  $M_X$  being the residual mass of all final particles in this semi-inclusive decay except the deuteron. For the semi-inclusive decays of  $\Upsilon(nS)$  to  $\bar{d}^*(2380)+X$ , the calculation can be carried out in the same way, but replacing the wave function and the mass of the deuteron with those of the  $d^*(2380)$ .

### 3 Numerical results and discussion

In this section, we will present the numerical results for the widths of the semi-inclusive decays  $\Upsilon(nS) \rightarrow \bar{d}(\bar{d}^*)+X$ . Before calculating the widths, we present the channel wave functions of deuteron and  $d^*(2380)$  (both  $\Delta\Delta$  and  $C_8C_8$  components) in Fig. 2.

In this figure, we only plot the wave functions in the  $S$  partial wave and ignore those in the  $D$  partial wave, because the latter is negligibly small. From these curves, one clearly sees that the size of  $d$  is larger than that of  $d^*$ , and the size of the  $C_8C_8$  component is even smaller. The peaks of the wave functions for the deuteron, the  $\Delta\Delta$

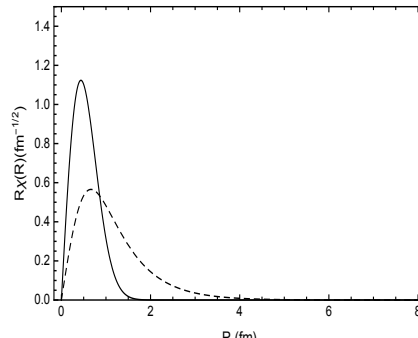


Fig. 2. Channel wave functions in the  $S$  partial wave by using the extended chiral SU(3) quark model. The solid curve in the left-hand diagram shows the wave function of the deuteron, and the dashed and solid curves in the right-hand diagram show the wave functions of the  $\Delta\Delta$  and  $C_8C_8$  components of  $d^*(2380)$ , respectively.

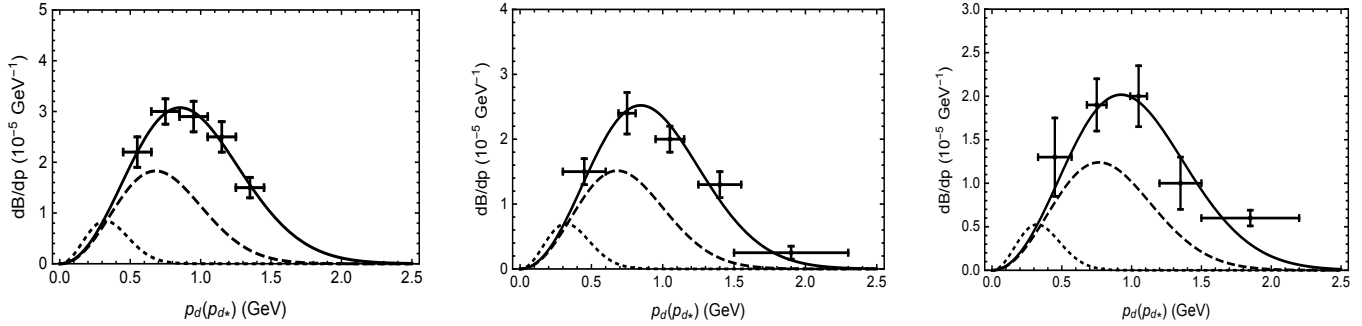


Fig. 3. The momentum distributions of  $\bar{d}$  ( $\bar{d}^*$ ) for the process  $\Upsilon(nS) \rightarrow \bar{d}(\bar{d}^*) + X$ . The figures, from left to right, are for decays of  $\Upsilon(1S)$ ,  $\Upsilon(2S)$  and  $\Upsilon(3S)$ , respectively. The dots are data observed in experiments. The solid lines are fits for  $\bar{d}$  and the dashed lines are predictions for  $\bar{d}^*$ .

and  $C_8C_8$  components of  $d^*$  are located around 1.5 fm, 0.8 fm and 0.5 fm, respectively.

With these wave functions and Eqs. (7)-(9), we are able to calculate the decay widths of  $\Upsilon(nS)$  to  $\bar{d}(\bar{d}^*) + X$ . We firstly calculate the widths of  $\Upsilon(nS)$  decaying to  $\bar{d} + X$  and compare them with the data to restrict the value of the coupling constant  $g_{\bar{b}qB}$ . As mentioned above, due to energy conservation, the maximal momentum of the deuteron should satisfy Eq. (10), namely it is residual mass dependent. However, in the semi-inclusive decay, the only affirmed information for  $X$  is its baryon number being 2, and the mass of  $X$  may have a value within a broad range of about 2–7 GeV. Therefore, the maximal value of  $p_d$ , and consequently the resultant decay widths, will vary according to the residual mass of  $M_X$ , or somehow relate to the momentum transfer  $\mathbf{q}$  (more momentum related content will be discussed later). To get a meaningful result, we treat this issue by inserting a phenomenological form factor of the  $p_d$  distribution:

$$F(p_d) = \mathcal{N} \exp \left[ -\frac{(p_d - p_0)^2}{\Lambda^2} \right], \quad (11)$$

where  $\mathcal{N}$  denotes the normalization factor,  $p_0$  is the most probable distribution point of  $p_d$ , and  $\Lambda$  describes the degree of the  $p_d$  extension. Therefore, in our calculation, there are three parameters,  $p_0$ ,  $\Lambda$ , and the coupling constant  $g_{\bar{b}qB}$ .  $p_0$  and  $\Lambda$  are determined by the experimental momentum distribution of the  $\bar{d}$  from the semi-inclusive processes  $\Upsilon(nS) \rightarrow \bar{d} + X$ .  $g_{\bar{b}qB}$  is determined by the experimental decay width data.

Inserting the above form factor into the original Eq. (9), we can get the final momentum distribution of  $\bar{d}$ . In Fig. 3, the momentum distribution of  $\bar{d}$  is shown by solid lines. The figures, from left to right, are for the decay of  $\Upsilon(1S)$ ,  $\Upsilon(2S)$  and  $\Upsilon(3S)$ , respectively. For example, for  $\Upsilon(1S)$ ,  $p_0$  and  $\Lambda$  are determined to be 0.24 GeV and 0.8 GeV, which provide the best fit to the experimental momentum distribution [25]. With the obtained  $p_0$  and  $\Lambda$ ,  $g_{\bar{b}qB}$  is determined to be  $2.5 \times 10^{-3}$  to

get the decay width of  $\Upsilon(1S) \rightarrow \bar{d} + X$   $154 \times 10^{-5}$  KeV. For  $\Upsilon(2S)$  and  $\Upsilon(3S)$ , from the experimental distributions [26],  $p_0/\Lambda$  are obtained as 0.25 GeV/0.78 GeV and 0.27 GeV/0.87 GeV, respectively.

It should be mentioned that in our model calculation,  $g_{\bar{b}qB}$  is considered phenomenologically as an effective coupling constant, instead of a momentum dependent one. In other words, we neither use a running coupling constant nor add a form factor to the vertex of the quark-meson interaction. Since the mass of  $\Upsilon(nS)$  increases with increasing main quantum number  $n$ , the momentum dependence of their semi-inclusive decay widths will also vary, namely the phenomenological coupling constants for different  $\Upsilon(nS)$  states should have certain deviations. To compensate for this difference, we determine the  $g_{\bar{b}qB}$  for different  $\Upsilon(nS)$  states by fitting their own observed decay widths. As a result, the obtained effective coupling constants  $g_{\bar{b}qB}(nS)$  for  $\Upsilon(2S)$  and  $\Upsilon(3S)$  are  $1.9 \times 10^{-3}$  and  $1.3 \times 10^{-3}$ , respectively. This is consistent with the result from the form factor method, where the effective coupling constant decreases with the increasing momentum.

With the determined effective coupling constants for corresponding  $\Upsilon(nS)$ , we can proceed with the calculations for the decay widths of the  $\Upsilon(nS) \rightarrow \bar{d}^*(2380) + X$  processes. In the calculation,  $g_{\bar{b}qB}(nS)$  for different  $nS$  states take the same values as those in the corresponding deuteron case. However, we have no information on the momentum distributions of the  $\bar{d}^*$ , i.e., we do not know the exact values of  $p_0$  and  $\Lambda$ . Since the mass of  $d^*$  is larger than that of the deuteron, one can imagine that  $p_0$  for the  $\bar{d}^*$  is smaller than that for  $\bar{d}$ . Therefore, in our calculation,  $p_0$  and  $\Lambda$  in the  $\bar{d}^*$  case are chosen properly to be in relatively large ranges. For example, for  $\Upsilon(nS)$ ,  $p_0$  is chosen to be in the range 0.05–0.2 GeV, which is smaller than that in the anti-deuteron case. The range of  $\Lambda$  is chosen to be 0.3–0.6 GeV for  $\Upsilon(1S)$  and  $\Upsilon(2S)$  and 0.3–0.7 GeV for  $\Upsilon(3S)$ . Similar to the  $\bar{d}$  case, for  $\bar{d}^*$ , the final momentum distributions are obtained by

inserting the form factors of  $\bar{d}^*$  into Eq. (9). The resultant momentum distributions are shown in Fig. 3 by dashed lines. The left-hand dashed line in each figure is for  $(p_0, \Lambda) = (0.05 \text{ GeV}, 0.3 \text{ GeV})$  and the right-hand dashed line is for  $(p_0, \Lambda) = (0.2 \text{ GeV}, 0.6 \text{ GeV} / 0.7 \text{ GeV}$  for  $\Upsilon(3S)$ ). It is found that the smaller the momentum of  $\bar{d}^*$ , the lower its production rate.

In Fig. 4, we show the decay widths of  $\Upsilon(nS) \rightarrow \bar{d}^* + X$  versus  $p_0$  and  $\Lambda$  using 3-dimensional figures. The figures, from left to right, correspond to  $\Upsilon(1S)$ ,  $\Upsilon(2S)$  and  $\Upsilon(3S)$ , respectively. From the figure, one can see that the decay widths increase with increasing  $p_0$  and  $\Lambda$ . For  $\Upsilon(1S)$ , the predicted range of width is from  $16 \times 10^{-5} \text{ keV}$  to  $71 \times 10^{-5} \text{ keV}$ . The smallest number is for  $p_0 = 0.05 \text{ GeV}$  and  $\Lambda = 0.3 \text{ GeV}$ , while the largest number is for  $p_0 = 0.2 \text{ GeV}$  and  $\Lambda = 0.6 \text{ GeV}$ . Compared with the decay width of  $\Upsilon(1S) \rightarrow \bar{d} + X$ , the production rate of  $\bar{d}^*$  is suppressed by about 2–10 times. For  $\Upsilon(2S)$  and  $\Upsilon(3S)$ , the widths

are in the ranges from  $9.6 \times 10^{-5} \text{ keV}$  to  $42 \times 10^{-5} \text{ keV}$  and  $4.4 \times 10^{-5} \text{ keV}$  to  $24 \times 10^{-5} \text{ keV}$ , which are also about 2–10 times smaller than the corresponding cases of  $\bar{d}$ . The production rates of  $\bar{d}^*$  are smaller than  $\bar{d}$ , mainly because of the mass difference between  $\bar{d}^*$  and  $\bar{d}$ . The difference of the wave functions has only a slight influence, though the shapes of their wave functions are quite different.

The calculated momentum of  $\bar{d}^*$  is likely in the range 0.3–0.8 GeV. Therefore, if we want to find  $\bar{d}^*$  in  $\Upsilon(nS)$  decays, we need to detect it in this momentum region. With the chosen parameter ranges, the production rate of  $\bar{d}^*$  is suppressed by 2–10 times compared with the corresponding production rate of  $\bar{d}$ . Finding  $\bar{d}^*$  is still within experimental ability [27]. However, if the momentum of  $\bar{d}^*$  is concentrated in an even smaller region due to some special mechanism,  $\bar{d}^*$  will be hard to discover from  $\Upsilon(nS)$  decays at current experimental facilities.

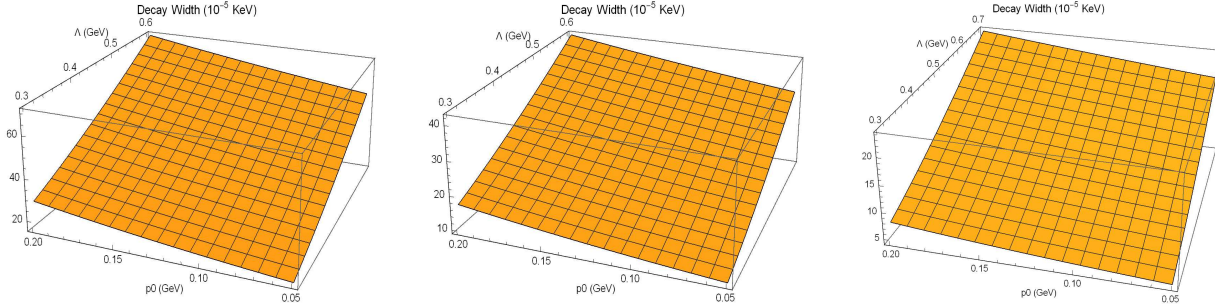


Fig. 4. (color online) The predicted decay widths of  $\Upsilon(nS) \rightarrow \bar{d}^* + X$  versus  $p_0$  and  $\Lambda$ . The figures, from left to right, are for  $\Upsilon(1S)$ ,  $\Upsilon(2S)$  and  $\Upsilon(3S)$ , respectively.

Table 1. The coupling constants, parameters of the momentum distribution, and decay widths for the process of  $\Upsilon(nS) \rightarrow \bar{d} (\bar{d}^*(2380)) + X$ .

state	$g_{\bar{d}qB}(10^{-3})$	$p_0^d/\text{GeV}$	$\Lambda^d/\text{GeV}$	$\Gamma_{\bar{d}}/(10^{-5} \text{ KeV})$	$p_0^{\bar{d}^*}/\text{GeV}$	$\Lambda^{\bar{d}^*}/\text{GeV}$	$\Gamma_{\bar{d}^*}/(10^{-5} \text{ KeV})$
1S	2.5	0.24	0.80	154	0.05–0.2	0.3–0.6	16–71
2S	1.9	0.25	0.78	89	0.05–0.2	0.3–0.6	9.6–42
3S	1.3	0.27	0.87	47	0.05–0.2	0.3–0.7	4.4–24

## 4 Summary

We calculated the widths of semi-inclusive decays of  $\Upsilon(nS) \rightarrow \bar{d}^*(2380) + X$ . With the help of crossing symmetry, the decay widths are obtained by investigating the imaginary part of the forward scattering amplitudes between  $d^*$  and  $\Upsilon(nS)$ . The wave functions of the deuteron and  $d^*$  are obtained from chiral SU(3) quark model calculations, and the wave functions of  $\Upsilon(nS)$  are calculated by solving the Schrödinger equation with a Cornell potential. In the  $\Upsilon(nS)$ - $d^*$  scattering, as a rough estimation, a  $s$ -channel B-meson exchange is assumed as a dominant interaction where the basic coupling con-

stant  $g_{\bar{d}qB}$  is phenomenologically determined by fitting the observed partial decay widths of the  $\Upsilon(nS) \rightarrow \bar{d} + X$  processes. To compensate for the lack of information about  $X$ , a Gaussian function is introduced and  $p_0$  and  $\Lambda$  in the function are obtained by reproducing the experimental momentum distributions of  $\bar{d}$ . For the  $\bar{d}^*$  cases, since we have no information on the momentum distribution of  $d^*$  in the final states, we study  $d^*$  in relatively large ranges for  $p_0$  and  $\Lambda$ . The calculated momentum of the generated  $\bar{d}^*$  is in the range 0.3–0.8 GeV. The overall widths of  $\Upsilon(nS)$  ( $n=1,2,3$ ) decaying into  $\bar{d}^* + X$  are about  $(16–71) \times 10^{-5} \text{ keV}$ ,  $(9.6–42) \times 10^{-5} \text{ keV}$ , and  $(4.4–24) \times 10^{-5} \text{ keV}$ , respectively, which are about 2–10

times smaller than those in the  $\bar{d}$  cases. It is still within experimental ability to find  $\bar{d}^*$  in  $\Upsilon(nS)$  decays. The difference in the wave functions between deuterons and  $d$  has only a tiny influence on the productions of  $d$  and  $\bar{d}^*$ . The suppression of the production rates of  $\bar{d}^*$  is mainly due to the mass difference (or phase space difference) between  $\bar{d}$  and  $\bar{d}^*$ . We summarize our obtained values of the coupling constants, parameters for momentum distribution, and decay widths in Table 1. The labels

$\bar{d}$  and  $\bar{d}^*$  are shown explicitly for these two cases. As a conclusion, it is very likely that one can find  $\bar{d}^*(2380)$  in the semi-inclusive decays of  $\Upsilon(nS)$ .

The authors thank F. Huang for providing the wave functions of the  $d^*$  and deuteron, and thank Z. X. Zhang, C. Z. Yuan and C. P. Shen for helpful discussions. Chao-Yi Lü is grateful to Yu Lu for suggestion on Mathematica.

## Appendices A

Jacobian transformations for the  $\Upsilon$ , nucleon and deuteron systems, respectively.

$$\begin{cases} \vec{p}_\eta = \frac{1}{2}(\vec{p}_b - \vec{p}_{\bar{b}}) \\ \vec{k} = (\vec{p}_b + \vec{p}_{\bar{b}}), \end{cases} \quad (A1)$$

$$\begin{cases} \vec{p}_\rho = \frac{1}{2}(\vec{p}_u - \vec{p}_{d_1}) \\ \vec{p}_\lambda = \frac{1}{3}(\vec{p}_u + \vec{p}_{d_1} - 2\vec{p}_{d_2}) \\ \vec{p}_n = (\vec{p}_u + \vec{p}_{d_1} + \vec{p}_{d_2}), \end{cases} \quad \begin{cases} \vec{p}_R = \frac{1}{2}(\vec{p}_n - \vec{p}_p) \\ \vec{p}_d = (\vec{p}_n + \vec{p}_p), \end{cases} \quad (A2)$$

where  $\vec{p}_\rho$ ,  $\vec{p}_\lambda$  and  $\vec{p}_n$  are the internal momenta of the nucleon, and internal momentum of  $\Upsilon$ , respectively.  $\vec{p}_n$  and  $\vec{k}$  represent the momenta of the nucleon and  $\Upsilon$ , respectively.  $\vec{p}_R$  denotes the relative momentum between nucleons, and  $\vec{p}_d$  is the center of mass momentum of the deuteron. The momenta on the right-hand side of the equations are those of the particles labeled by the subscripts.

## References

- 1 M. Bashkanov et al, Phys. Rev. Lett., **102**: 052301 (2009)
- 2 P. Adlarson et al, Phys. Rev. Lett., **106**: 242302 (2011)
- 3 S. Keleta et al, Nucl. Phys. A, **825**: 71 (2009)
- 4 P. Adlarson et al (WASA-at-COSY Collaboration), Phys. Rev. C, **86**: 032201 (2012)
- 5 P. Adlarson et al (WASA-at-COSY Collaboration), Phys. Rev. C, **88**: 055208 (2013)
- 6 P. Adlarson et al (WASA-at-COSY Collaboration), Phys. Lett. B, **743**: 325 (2015)
- 7 P. Adlarson et al (WASA-at-COSY Collaboration), Phys. Rev. C, **91**: 015201 (2015)
- 8 P. Adlarson et al (WASA-at-COSY Collaboration), Phys. Rev. Lett., **112**: 202301 (2014)
- 9 H. Clement, Progress in Particle and Nuclear Physics, **93**: 195 (2017)
- 10 X. Q. Yuan, Z. Y. Zhang, Y. W. Yu, and P. N. Shen, Phys. Rev. C, **60**: 045203 (1999)
- 11 M. Bashkanov, S. J. Brodsky, and H. Clement, Phys. Lett. B, **727**: 438 (2013)
- 12 F. Huang, Z. Y. Zhang, P. N. Shen, and W. L. Wang, Chin. Phys. C, **39**(7): 071001 (2015)
- 13 Y. B. Dong, P. N. Shen, F. Huang, and Z. Y. Zhang, Phys. Rev. C, **91**(6): 064002 (2015)
- 14 Y. B. Dong, F. Huang, P. N. Shen, and Z. Y. Zhang, Phys. Rev. C, **94**(1): 014003 (2016)
- 15 Y. B. Dong, F. Huang, P. N. Shen, and Z. Y. Zhang, Phys. Lett. B, **769**: 223 (2017)
- 16 Y. B. Dong, F. Huang, P. N. Shen, and Z. Y. Zhang, Phys. Rev. D, **96**: 094001 (2017)
- 17 A. Gal and H. Garcilazo, Phys. Rev. Lett., **111**: 172301 (2013)
- 18 A. Gal and H. Garcilazo, Nucl. Phys. A, **928**: 73 (2014)
- 19 C. Patrignani et al (Particle Data Group), Chin. Phys. C, **40**(10): 100001 (2016)
- 20 E. Eichten, K. Gottfried, T. Kinoshita, K. D. Lane, and T. M. Yan, Phys. Rev. D, **21**: 203 (1980)
- 21 Y. B. Ding, X. Q. Li, and P. N. Shen, Phys. Rev. D, **60**: 074010 (1999)
- 22 Y. Lu, M. N. Anwar, and B. S. Zou, Phys. Rev. D, **94**: 034021 (2016)
- 23 Y. Lu, M. N. Anwar, and B. S. Zou, Phys. Rev. D, **95**: 034018 (2017)
- 24 F. Huang, P. N. Shen, Y. B. Dong, and Z. Y. Zhang, Sci. China Phys. Mech. Astron., **59**(2): 622002 (2016)
- 25 D. M. Asner et al, Phys. Rev. D, **75**: 012009 (2007)
- 26 J. P. Lees et al, Phys. Rev. D, **89**: 111102 (R) (2014)
- 27 Private discussion with experimentalists